

TinyML NLP Approach for Semantic Wireless Sentiment Classification

Ahmed Y. Radwan¹, Mohammad Shehab², and Mohamed-Slim Alouini²

¹Department of Electrical Engineering and Computer Science, York University, Toronto, ON M3J 1P3, Canada

²CEMSE Division, King Abdullah University of Science and Technology (KAUST), Thuwal 23955-6900, Saudi Arabia

Email: ahmedyra@yorku.ca

Abstract—Natural Language Processing (NLP) operations, such as semantic sentiment analysis and text synthesis, may often impair users privacy and demand significant on device computational resources. Centralized learning (CL) on the edge offer alternative energy efficient approach, yet requires the collection of raw information, which affects the users privacy. While Federated learning (FL) preserves privacy, it requires high computational energy on board tiny user devices. We introduce split learning (SL) as an energy efficient alternative, privacy preserving tiny machine learning (TinyML) scheme and compare it to FL and CL in the presence Rayleigh fading and additive noise. Our results show that SL reduces processing power and CO₂ emissions while maintaining high accuracy, whereas FL offers a balanced compromise between efficiency and privacy. Hence, this study provides insights into deploying energy-efficient, privacy-preserving NLP models on edge devices.

Index Terms—Federated learning, split learning, TinyML, semantic communication, NLP.

I. INTRODUCTION

Artificial Intelligence (AI) has gained widespread adoption, with applications ranging from text and image classification to text and image generation. A key area of growth is NLP, which powers virtual assistants and human language classification systems. Large language models (LLMs), such as OpenAI’s GPT series [1], Gemini [2], and BERT, built on Transformer architectures [3], have transformed NLP by enabling machines to perform complex language tasks with high accuracy. However, these models require significant computational resources for both training and inference, posing challenges for deployment on resource-constrained devices.

LLMs demand substantial storage and processing power. The high dimensionality of language data and large vocabularies further increase the computational burden [4]. Data privacy is another significant concern, as training robust models often requires diverse datasets, which can raise issues when handling sensitive information, such as in healthcare or government sectors. Additionally, deploying models on edge devices introduces communication challenges. Wireless data transmission over channels like WiFi is susceptible to noise, fading, limited bandwidth and unstable connections, which may affect communication efficiency.

TinyML mixed models have evolved to address the above concerns. For instance, model compression techniques, such as pruning [5], quantization [6], and knowledge distillation [7], help reduce model sizes and computational requirements.

TinyBERT [8] and MobileBERT [9], for example, utilize knowledge distillation to create smaller models, while quantization techniques, like in LLaMA [10], enable efficient execution on low-resource devices. FL offers a decentralized model training approach, allowing multiple users to collaboratively train a global model while keeping their data local. Although, this method addresses data privacy concerns [11], it might be power hungry for tiny device batteries. To this end, SL [12] divides the model training process between users and a server. Users transmit activations from the initial model layers, reducing computational load and enhancing data privacy.

In this paper, we propose two frameworks to address computational challenges and privacy concerns in text emotion classification: one based on FL and the other on SL. First, we focus on semantic extraction by utilizing quantization to significantly reduce model size, enabling deployment on resource-limited devices. Second, we emphasize privacy preservation by ensuring that data remains on the device while transmitting only the necessary information for model training. The proposed methods prove robustness in challenging channel conditions while reducing the overall energy consumption and CO₂ emissions, contributing to TinyML initiatives.

The remainder of this paper is structured as follows: Section II covers the system design and experimental setup, including both frameworks of FL and SL techniques. Section III presents the experimental results, focusing on accuracy, energy consumption, and the impact of noise and fading. Finally, Section IV provides conclusions and discusses potential directions for future work.

II. SYSTEM LAYOUT

A. Federated Learning System

As shown in Fig 1, in FL, N users collaborate by training local models and sharing their updates with a central server over K communication cycles. The key operation in FL is the transmission of quantized model updates to minimize communication overhead and ensure data privacy, as raw data never leaves the users’ devices. As shown in Fig. 1, each communication cycle k involves several key steps. Each user i performs J local training iterations on their private dataset to update their local model weights $W_i^{(k)}$. This iterative local training allows users to improve their models before sharing updates with the server. The updated local model weights

Cycle of Federated Learning

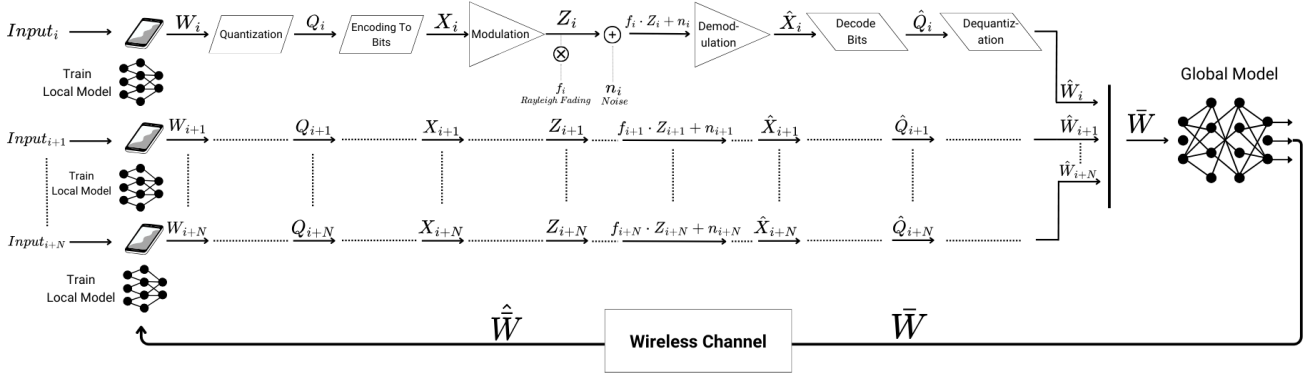


Fig. 1: Federated learning system design

$W_i^{(k)}$ are quantized to reduce communication overhead. The quantization process converts the weights into discrete levels, scaled by a factor $S_i^{(k)}$ derived from the maximum absolute weight value and the bit-width b used for quantization. The quantized weights $Q_i^{(k)}$ are computed as:

$$Q_i^{(k)} = \left\lfloor \frac{W_i^{(k)}}{S_i^{(k)}} \right\rfloor, \quad (1)$$

where the scale factor $S_i^{(k)}$ is defined as:

$$S_i^{(k)} = \frac{\max(|W_i^{(k)}|)}{2^{b-1} - 1}. \quad (2)$$

After quantization, the quantized weights $Q_i^{(k)}$ are encoded into a bit stream $X_i^{(k)}$, which is then digitally modulated into a signal $Z_i^{(k)}$. This signal is transmitted through the wireless channel. Consequently, the received signal $\hat{Z}_i^{(k)}$ is a faded and noisy version of the originally transmitted signal due to Rayleigh fading $f_i^{(k)}$ and additive noise $n_i^{(k)}$. These channel effects can lead to slight changes in the demodulated bit stream $\hat{X}_i^{(k)}$ [13]. The server then collects the received updates $\hat{Z}_i^{(k)}$ from each user i . These signals are first demodulated into the bit stream $\hat{X}_i^{(k)}$, which is then decoded into the quantized weights $\hat{Q}_i^{(k)}$. After decoding, the server dequantizes $\hat{Q}_i^{(k)}$ to recover the estimated model weights $\hat{W}_i^{(k)}$

$$\hat{W}_i^{(k)} = \hat{Q}_i^{(k)} \cdot S_i^{(k)}. \quad (3)$$

Finally, the server aggregates these dequantized updates using Federated Averaging (FedAvg) [14] as

$$\bar{W}^{(k+1)} = \frac{1}{N} \sum_{i=1}^N \hat{W}_i^{(k)}. \quad (4)$$

Here, $\bar{W}^{(k+1)}$ represents the updated global model after aggregating the users' contributions. The server then broadcasts $\bar{W}^{(k+1)}$ back to the users, who update their local models accordingly for the next cycle

$$W_i^{(k+1)} = \bar{W}^{(k+1)}. \quad (5)$$

This process is repeated for K communication cycles, allowing the global model to converge through iterative refinement while maintaining data privacy. The whole FL process is summarized in Algorithm 1.

B. Split Learning System

SL enables a distributed learning approach where the model is divided between a user and a server, as shown in Fig. 2. In each communication cycle k , the user processes only the initial layers of the model locally, which reduces the computational burden on the user and helps protect raw data privacy. Then, it transmits the intermediate activations to the server for further processing. Specifically, for a given input x_i at cycle k , the user computes the smashed data

$$S_i^{(k)} = f_{\text{user}}(x_i; W_{\text{user}}^{(k)}), \quad (6)$$

where $W_{\text{user}}^{(k)}$ are the user-side model weights at cycle k , and $S_i^{(k)}$ represents the output of the user's model partition (i.e., smashed data). The output $S_i^{(k)}$ is first encoded into bits $X_i^{(k)}$ and then digitally modulated into a signal $Z_i^{(k)}$. This signal is transmitted through the wireless channel as will be defined in Section II-C. Due to channel effects, errors can be introduced in the received signal, affecting the accuracy of the demodulated bit stream $\hat{X}_i^{(k)}$. Upon receiving the noisy signal, the server demodulates and decodes it to obtain the estimated activations $\hat{S}_i^{(k)}$, which are then utilized to complete the forward pass

$$\hat{y}_i^{(k)} = f_{\text{server}}(\hat{S}_i^{(k)}; W_{\text{server}}^{(k)}), \quad (7)$$

where $W_{\text{server}}^{(k)}$ are the server-side model weights at cycle k , and $\hat{y}_i^{(k)}$ is the server's output prediction. The loss function is computed as

$$L^{(k)} = \mathcal{L}(\hat{y}_i^{(k)}, y_i), \quad (8)$$

where y_i is the ground truth label, and \mathcal{L} denotes the loss function (e.g., cross-entropy loss).

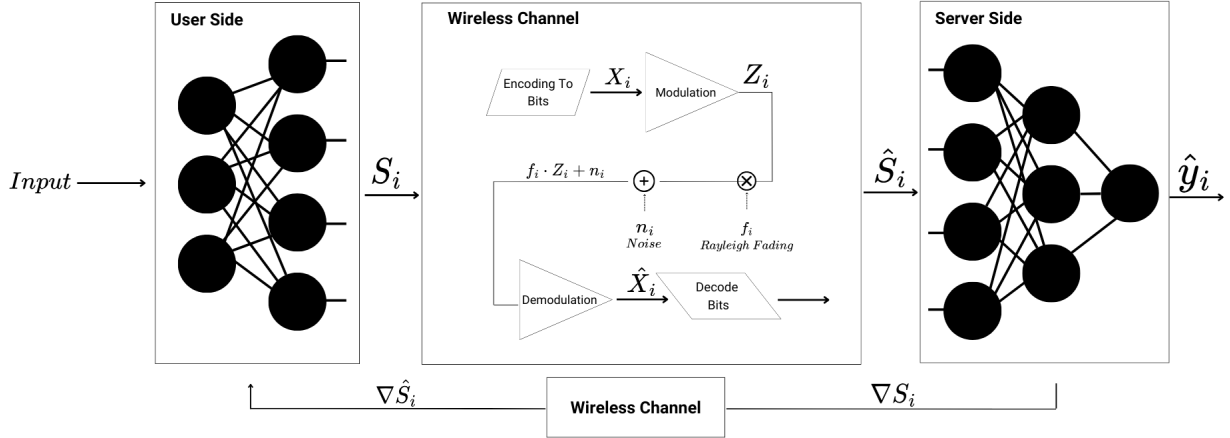


Fig. 2: Split learning system design for one user. The user processes the initial layers and sends intermediate activations to the server for further processing.

The server computes gradients with respect to its model weights and the activations. The gradient $\nabla_{\hat{S}_i^{(k)}} L^{(k)}$ is clipped to manage its magnitude and then transmitted back to the user through the wireless channel. The clipped gradient is encoded into bits, modulated using BPSK, and affected by channel impairments similar to the forward transmission. The server updates its model weights using

$$W_{\text{server}}^{(k+1)} = W_{\text{server}}^{(k)} - \eta \nabla_{W_{\text{server}}^{(k)}} L^{(k)}, \quad (9)$$

where η is the learning rate. The user receives the noisy version of the gradients, demodulates and decodes them to obtain the estimated gradients $\widehat{\nabla}_{\hat{S}_i^{(k)}} L^{(k)}$, and then performs backpropagation on the local layers to compute $\nabla_{W_{\text{user}}^{(k)}} L^{(k)}$. The user updates its model weights as

$$W_{\text{user}}^{(k+1)} = W_{\text{user}}^{(k)} - \eta \nabla_{W_{\text{user}}^{(k)}} L^{(k)}. \quad (10)$$

This process is repeated over K communication cycles, allowing both the user and server models to improve, iteratively. The process of SL is summarized in Algorithm 2.

C. Wireless Channel

In both learning systems, semantically encoded model updates or activations (denoted as Z) are transmitted over wireless channels subject to Rayleigh fading and additive white Gaussian noise (AWGN). The fading and noise models are respectively defined as

$$f = \sqrt{X^2 + Y^2}, \quad X, Y \sim N(0, 1), \quad (11)$$

$$n \sim N(0, \sigma^2). \quad (12)$$

The fading coefficient f uniformly affects all transmitted signals Z_i , and the noisy transmission is represented by

$$\hat{Z} = f \cdot Z + n, \quad (13)$$

and similar definitions apply for the feedback in both cases.

Algorithm 1 Federated Learning for Semantic Wireless Text Sentiment Classification

- 1: **Initialize:** $\eta, J, K, \sigma^2, Q, N, \hat{\mathbf{W}}^{(0)}$
- 2: **for** $k = 1$ to K **do**
- 3: **for** $i = 1$ to N **do**
- 4: **User i :**
- 5: $W_i^{(k)} = \hat{\mathbf{W}}^{(k)}$
- 6: **for** $j = 1$ to J **do**
- 7: $W_i^{(k)} \leftarrow W_i^{(k)} - \eta \nabla L_i(W_i^{(k)})$
- 8: **end for**
- 9: $Q_i^{(k)} = \text{Quantize}(W_i^{(k)}, Q)$ {Using (1) (2)}
- 10: $X_i^{(k)} = \text{Encode}(Q_i^{(k)})$
- 11: $Z_i^{(k)} = \text{Modulate}(X_i^{(k)})$
- 12: Transmit: $\tilde{Z}_i^{(k)} = f_i \cdot Z_i^{(k)} + n_i$, using (11) (12) (13)
- 13: **end for**
- 14: **Server:**
- 15: $\hat{Z}_i^{(k)} = \text{Demodulate}(\tilde{Z}_i^{(k)}) \forall i$
- 16: $\hat{X}_i^{(k)} = \text{Decode}(\hat{Z}_i^{(k)}) \forall i$
- 17: $\hat{Q}_i^{(k)} = \text{Dequantize}(\hat{X}_i^{(k)}) \forall i$
- 18: Obtain $\bar{W}^{(k+1)}$ using Using (4) and broadcast it to back all users.
- 19: **end for**

D. Communication Energy Calculation

In our approach, communication energy is determined by calculating the channel capacity C , which represents the maximum data rate for error-free transmission. Using the Shannon-Hartley theorem [15], the channel capacity incorporates both the Signal-to-Noise Ratio (SNR) and the bandwidth B . The time required to transmit one bit and the corresponding energy consumption per bit is derived from the following equations. The SNR, representing the ratio of signal power P to noise power σ^2 , is given by

$$\text{SNR} = \frac{P}{\sigma^2}. \quad (14)$$

Algorithm 2 Split Learning for Semantic Wireless Text Sentiment Classification

```

1: Initialize:  $\eta, K, \sigma^2, L, N, \tau, W_{\text{user}}^{(0)}, W_{\text{server}}^{(0)}$ 
2: for  $k = 1$  to  $K$  do
3:   for  $i = 1$  to  $N$  do
4:     User  $i$ :
5:     Compute  $S_i^{(k)} \leftarrow \text{UserOutput}(W_{\text{user}}^{(k)})$  {Eq. (6)}
6:     Transmit  $\tilde{Z}_i^{(k)}$  {Encoding, Modulation; Using (11), (12), (13)}
7:   end for
8:   Server:
9:   Compute  $\hat{y}_i^{(k)} \leftarrow \text{ServerProcess}(\tilde{Z}_i^{(k)})$  {Decode, De-modulate; Using (7)}
10:  Compute loss  $L \leftarrow \text{LossFunction}(\hat{y}_i^{(k)}, y_i)$  {Using (8)}
11:  Clip gradients  $g_{\text{server}}^{\text{clipped}} \leftarrow \text{clip}_{\text{norm}}(\nabla L_{\text{server}}, \tau)$ 
12:  Update  $W_{\text{server}}^{(k+1)}$  {Eq. (9)}
13:  Compute gradients  $\nabla S_i^{(k)} \leftarrow \nabla \text{UserOutput}(W_{\text{user}}^{(k)})$ 
14:  Transmit gradient  $\tilde{Z}_{\nabla i}^{(k)}$  {Encoding, Modulation; Using (11), (12), (13)}
15:  for  $i = 1$  to  $N$  do
16:    User  $i$ :
17:    Clip user gradients  $g_{\text{user}}^{\text{clipped}} \leftarrow \text{clip}_{\text{norm}}(\widehat{\nabla S_i^{(k)}} \cdot \nabla W_{\text{user}}^{(k)}, \tau)$ 
18:    Update  $W_{\text{user}}^{(k+1)}$  {Using (10)}
19:  end for
20: end for

```

Here, P is the transmission power and σ^2 is the noise variance as defined in (12). These parameters are utilized in both FL and SL systems. Next, the channel capacity C is computed as

$$C = B \log_2(1 + \text{SNR}). \quad (15)$$

Finally, the energy consumed per transmitted bit is given by

$$\text{Energy per Bit} = \frac{P}{C} J/b, \quad (16)$$

which is multiplied by the total number of bits (payload) to estimate the consumed communication energy.

III. EXPERIMENTS AND RESULTS

We conducted our experiments using the Sentiment140 dataset [16], [17], which contains 1.6 million tweets. To adapt the dataset for resource-constrained devices, only the text and target labels (0 for negative sentiment and 1 for positive sentiment) were retained, and the dataset size was halved. All experimental configurations are summarized in Table I. Specifically, 90% of the data was allocated for training and 10% for testing. The vocabulary was restricted to the 10,000 most frequent words, and the maximum sequence length was set to 30. We employed 3 users in the FL setup and 1 global, undergoing 7 communication cycles with a batch size of 512. user models were trained for 5 epochs per user per cycle. Binary phase shift keying (BPSK) is the digital

TABLE I: Experimental Parameters

Parameter	FL	SL
Training-Testing Split	90% training, 10% testing	
Vocabulary Size	10,000 most frequent words	
Maximum Sequence Length	30	
Number of Users	3	1
Communication Cycles	7 cycles, 5 epochs/user	50 cycles
Batch Size	512	
Optimizer	SGD	
Momentum	0.9	
Initial Learning Rate	0.01	
Learning Rate Scheduler	Reduce by 10% every 5 epochs	
Gradient Clipping Threshold	-	0.5
Bandwidth	100 KHz	

modulation scheme adopted to transmit the quantized data. Energy consumption and CO₂ emissions were monitored using the Eco2AI framework [18], with measurements taken every 10 seconds during the FL cycles.

In the CL setup, 3 users collaborated in sending the data to the server, and the SL setup involved one user and one server. Both CL and FL models were trained for 50 cycles using the same batch size across all experiments. In SL, the model was partitioned at a specific split layer L , where convolutional and pooling layers were executed on the user's device to minimize computational complexity, while the rest of the layers were handled by the server. The update rules for the SGD optimizer are defined as

$$v_{t+1} = \mu \cdot v_t + \eta \cdot \nabla \mathcal{L}(w_t), \quad (17)$$

$$w_{t+1} = w_t - v_{t+1}. \quad (18)$$

To ensure stable training and prevent exploding gradients, gradient clipping was applied with a threshold of $\tau = 0.5$. If the gradient norm exceeded τ , it was scaled down to maintain the norm at or below this threshold as shown in Algorithm. 2. Gradient clipping stabilized the update steps, preventing large parameter changes that could destabilize convergence.

A. Model Architecture

The model, with a total of 89,673 parameters and an approximate size of 175.14 KB using 16-bit precision, is tailored for resource-constrained environments. This compact design, combined with our dual-approach framework, offers significant benefits in resource utilization and privacy protection.

1) *Federated learning:* The FL architecture consists of several layers: an input layer that accepts fixed-length sequences of maximum length N , an embedding layer that transforms input sequences into dense vectors of size 8, a convolutional layer with 32 filters and a kernel size of 3. After that comes batch normalization and max pooling, an LSTM layer with 32 units to capture temporal dependencies in the sequential output, a dense layer with 16 units using ReLU activation and L2 regularization, and finally, an output layer with 1 unit using sigmoid activation for binary classification.

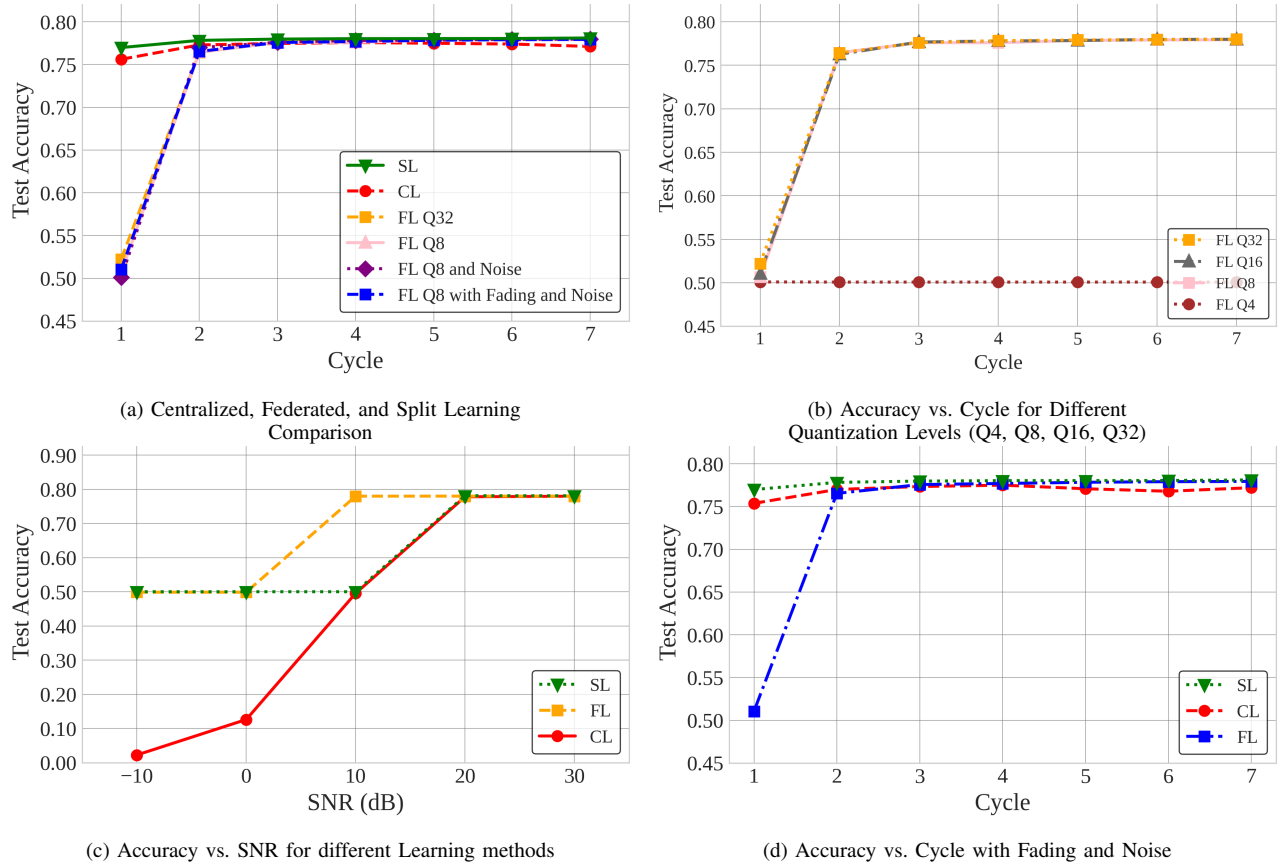


Fig. 3: Comparative analysis of learning methods: (a) centralized, federated, and split learning comparison; (b) Accuracy vs. cycle for different quantizations; (c) Accuracy vs. SNR in different learning methods; (d) Accuracy vs. cycle fading and noise.

2) *Split learning*: In SL the model is divided between the user and the server to reduce computational demands. The user-side computation is represented by the function $f_u(x)$, where x is the input data processed through the initial layers of the model, including convolutional and pooling layers. The output of $f_u(x)$ is then sent to the server, where the server-side computation $f_s(f_u(x)) = y$ processes the data further using the LSTM and subsequent layers to produce the final output y . This split allows the server to handle the more computationally intensive tasks, thereby completing the training process efficiently.

B. Experimental Results

Our experiments are designed to evaluate and compare various learning frameworks based on three key aspects: model accuracy, computational energy consumption, and communication energy consumption. We also investigate the effects of noise and Rayleigh fading.

As shown in Fig. 3a, both CL and FL with 8-bit (Q8) and 32-bit (Q32) quantization stabilize around an accuracy of 0.78. However, introducing noise with an SNR level of 20 dB and fading in CL as shown in Fig. 3d causes a slight degradation in accuracy. This degradation occurs because CL transmits raw data, which is directly impacted by noise and fading during transmission, leading to higher error

rates. In contrast, FL transmits quantized model weights, which are less vulnerable to transmission impairments due to their smaller size and structured form. This enables FL to maintain higher robustness. We also assess the impact of different quantization levels (Q4, Q8, Q16, and Q32) on model performance as shown in Fig. 3b. Lower-quantization levels (i.e., higher compression ratio) such as Q4 significantly reduce accuracy due to the loss of precision. In contrast, Q8 and higher provide a reasonable trade-off between accuracy and communication efficiency. Among the quantization levels tested, Q8 emerges as the optimal choice for FL, balancing accuracy and communication efficiency.

In Fig. 3c, we analyze the effect of varying SNR on model accuracy across FL, CL, and SL. Accuracy improves steadily with increasing SNR, particularly between 0 dB and 10 dB, with FL achieving the highest overall accuracy. Beyond 20 dB, accuracy plateaus at about 0.78 across all methods, with 20 dB identified as a reasonable balance between accuracy and communication power. Again, FL is more robust in noisy and fading environments. Meanwhile, Fig. 3d elucidates the effect of Rayleigh fading and noise together. Herein, we set the SNR to 20 dB. We observe that both FL with and SL with Q8 maintain high accuracy despite the challenging conditions, demonstrating their robustness in real-world scenarios, despite the communication channel

TABLE II: Accuracy, computation and communication energy, carbon footprints, and total bits transferred per cycle

Algorithm	Accuracy	Comp. Energy (J)	CO ₂ Emissions (g)	Comm. Energy (J)	Total Bits (M bits)
Central	0.7803	0	21.3	2.63	115.7
FL Q8	0.7806	60.82	9.64	1.64×10^{-3}	0.72
SL (Early Cut)	0.7813	2.95	0.47	23.5	10321.9

Note: Total Bits are reported per user. For all entries, computational energy is reported for the user side.

imperfections.

Finally, Table II summarizes each approach’s user-side energy usage and CO₂ emissions. Specifically, SL and FL were evaluated at a signal-to-noise ratio (SNR) of 20 dB, as indicated in the last three entries of the table. It is important to note that the table presents only the computational energy consumed on the user side. Consequently, CL appears with zero user-side computational energy consumption. However, CL incurs substantial energy usage on the server side, which is not reflected in this table.

While SL is highly efficient in terms of user-side computational power, utilizing only 3 J compared to CL’s 134 J on the server side and 61 J for FL, SL incurs the highest communication energy costs due to the frequent transmission of intermediate activations. FL achieves a balance between communication and computing efficiency, making it ideal for contexts with limited communication resources. Since computational energy on the user side is dominant over communication energy in federated and split learning approaches, these methods consume less energy on the user side in general. Specifically, SL is the most user-side energy-efficient and environment friendly in terms of CO₂ emissions making it an attractive TinyML solution.

IV. ENDLINE

We explored TinyML approaches for Semantic text sentiment classification via FL and SL. Our approaches are designed to be energy-efficient and privacy preserving alternatives to CL. It is clear that quantization techniques such as 8-bit quantization appeared to be optimum in our scenario. SL excels in reducing user-side computation and CO₂ emissions, while maintaining accuracy in noisy conditions but incurs higher communication energy. FL, especially with Q8 quantization, offers an optimal balance between computational efficiency, communication cost, and data privacy, making it ideal for decentralized environments with limited bandwidth. The proposed TinyML SL and FL approaches are considered very efficient for tiny devices with limited energy resources, where SL is the most energy efficient and environment friendly. Future work could explore differential privacy to improve efficiency and security.

REFERENCES

- [1] OpenAI, “Gpt-4 technical report,” *ArXiv*, vol. abs/2303.08774, 2023. [Online]. Available: <https://arxiv.org/abs/2303.08774>
- [2] J. Smith, J. Doe, A. Lee, and D. Kim, “Gemini: A large-scale multimodal model,” *ArXiv*, vol. abs/2312.11805, 2023. [Online]. Available: <https://arxiv.org/abs/2312.11805>
- [3] A. Vaswani, N. Shazeer, N. Parmar, J. Uszkoreit, L. Jones, A. N. Gomez, L. Kaiser, and I. Polosukhin, “Attention is all you need,” in *Proceedings of the 31st International Conference on Neural Information Processing Systems (NIPS)*, vol. 30, 2017, pp. 6000–6010. [Online]. Available: <https://arxiv.org/abs/1706.03762>
- [4] J. Lin, L. Zhu, W.-M. Chen, W.-C. Wang, and S. Han, “Tiny machine learning: progress and futures [feature],” *IEEE Circuits and Systems Magazine*, vol. 23, no. 3, pp. 8–34, 2023.
- [5] R. Reed, “Pruning algorithms—a survey,” *IEEE transactions on Neural Networks*, vol. 4, no. 5, pp. 740–747, 1993.
- [6] R. M. Gray and D. L. Neuhoff, “Quantization,” *IEEE Transactions on Information Theory*, vol. 44, no. 6, pp. 2325–2383, 1998. [Online]. Available: <https://doi.org/10.1109/18.720541>
- [7] J. Gou, B. Yu, S. J. Maybank, and D. Tao, “Knowledge distillation: A survey,” *International Journal of Computer Vision*, vol. 129, no. 6, pp. 1789–1819, 2021. [Online]. Available: <https://link.springer.com/article/10.1007/s11263-021-01453-z>
- [8] X. Jiao, Y. Yin, L. Shang, X. Jiang, X. Chen, L. Li, F. Wang, and Q. Liu, “Tinybert: Distilling bert for natural language understanding,” in *Proceedings of the 2020 Conference on Empirical Methods in Natural Language Processing (EMNLP)*, 2020, pp. 4163–4174. [Online]. Available: <https://www.aclweb.org/anthology/2020.emnlp-main.346>
- [9] Z. Sun, H. Yu, X. Song, R. Liu, Y. Yang, and D. Zhou, “Mobilebert: a compact task-agnostic bert for resource-limited devices,” in *Proceedings of the 58th Annual Meeting of the Association for Computational Linguistics (ACL)*, 2020, pp. 2158–2170. [Online]. Available: <https://www.aclweb.org/anthology/2020.acl-main.195>
- [10] H. Touvron, T. Lavril, G. Izacard, X. Martinet, M.-A. Lachaux, T. Lacroix, B. Rozière, N. Goyal, E. Hambro, F. Azhar *et al.*, “Llama: Open and efficient foundation language models,” *arXiv preprint arXiv:2302.13971*, 2023.
- [11] K. Kopparapu, E. Lin, J. G. Breslin, and B. Sudharsan, “Tinyfedtl: Federated transfer learning on ubiquitous tiny iot devices,” in *2022 IEEE International Conference on Pervasive Computing and Communications Workshops and other Affiliated Events (PerCom Workshops)*. IEEE, 2022, pp. 79–81.
- [12] P. Vepakomma, O. Gupta, T. Swedish, and R. Raskar, “Split learning for health: Distributed deep learning without sharing raw patient data,” *arXiv preprint arXiv:1812.00564*, 2018.
- [13] B. Xiao, X. Yu, W. Ni, X. Wang, and H. V. Poor, “Over-the-air federated learning: Status quo, open challenges, and future directions,” *Fundamental Research*, 2024.
- [14] A. Nilsson, S. Smith, G. Ulm, E. Gustavsson, and M. Jirstrand, “A performance evaluation of federated learning algorithms,” in *Proceedings of the second workshop on distributed infrastructures for deep learning*, 2018, pp. 1–8.
- [15] C. E. Shannon, “Communication theory of secrecy systems,” *The Bell system technical journal*, vol. 28, no. 4, pp. 656–715, 1949.
- [16] A. Go, R. Bhayani, and L. Huang, “Twitter sentiment classification using distant supervision,” *CS224N project report, Stanford*, vol. 1, no. 12, p. 2009, 2009.
- [17] A. Kazanov, “Sentiment140 dataset with 1.6 million tweets,” 2017, kaggle. [Online]. Available: <https://www.kaggle.com/datasets/kazanov/sentiment140>
- [18] S. A. Budenny, V. D. Lazarev, N. N. Zakharenko, A. N. Korovin, O. Plosskaya, D. V. Dimitrov, V. Akhripkin, I. Pavlov, I. V. Oseledets, I. S. Barsola *et al.*, “Eco2ai: carbon emissions tracking of machine learning models as the first step towards sustainable ai,” in *Doklady Mathematics*, vol. 106, no. Suppl 1. Springer, 2022, pp. S118–S128.